

Role of Pr cations and the low temperature transition in $\text{Pr}_{0.50}\text{Sr}_{0.50}\text{CoO}_3$: a comparison to $\text{Pr}_{0.50}\text{Ca}_{0.50}\text{CoO}_3$

J. Padilla-Pantoja^a, A. J. Barón-González^{a,b}, B. Bozzo^a, J. Blasco^c, C. Ritter^d, J. Herrero-Martín^e and J.L. García-Muñoz^a

^a*Institut de Ciència de Materials de Barcelona, ICMAB-CSIC, Campus Univ. de Bellaterra, E-08193 Bellaterra, Spain*

^b*Grupo Física de Materiales, Universidad Pedagógica y Tecnológica de Colombia, Tunja, Colombia.*

^c*Instituto de Ciencia de Materiales de Aragón, CSIC-Univ. de Zaragoza, 50009 Zaragoza, Spain*

^d*Institute Laue Langevin, BP 156, 38042 Grenoble Cedex 9, France.*

^e*ALBA Synchrotron Light Source, 08290 Cerdanyola del Vallès, Barcelona, Spain*

Abstract.

The low temperature properties of $\text{Pr}_{0.50}\text{Sr}_{0.50}\text{CoO}_3$ are studied in comparison to $\text{Pr}_{0.50}\text{Ca}_{0.50}\text{CoO}_3$, known to exhibit a $\text{Pr}^{3+}/\text{Pr}^{4+}$ valence shift below $T_{\text{MI}} \sim 80$ K. The evolution of the Pr-O network strongly differs in the Sr and Ca compounds, but both have in common a prominent and sudden contraction of some Pr-O bonds. The structural phase transition that accompanies the so-called magnetocrystalline anisotropy transition at $T_S \sim 120$ K in $\text{Pr}_{0.50}\text{Sr}_{0.50}\text{CoO}_3$ brings about a notable contraction of some Pr-O2 bonds. The observations give support to the active participation of Pr-4*f* electrons at the intriguing magnetostructural transition (T_S) in $\text{Pr}_{0.50}\text{Sr}_{0.50}\text{CoO}_3$. In addition, we have confirmed that (in absence of praseodymium) the magnetostructural transition is suppressed in $(\text{Nd}_{2/3}\text{La}_{1/3})_{0.50}\text{Sr}_{0.50}\text{CoO}_3$, a perovskite with the same average cationic size at the A-site than $\text{Pr}_{0.50}\text{Sr}_{0.50}\text{CoO}_3$.

Keywords: Cobaltites; Magnetocrystalline anisotropy; Ferromagnetism; Metallic perovskites

PACS: 71.30.+h, 61.05.fm, 75.30.Kz, 75.47.De

I. INTRODUCTION

Electronic transport properties and metal-insulator transitions (MIT) in cobaltites are attracting great interest due to the relevance of the spin state of Co for electron mobility in these strongly correlated oxides. In particular, some unusual properties in cobaltites containing trivalent cobalt are stimulated by the comparable energies of its crystal field and intra-atomic electron-electron coupling. The physical properties of half-doped $\text{Pr}_{0.50}\text{A}_{0.50}\text{CoO}_3$ (A: Ca or Sr) perovskites are a good example of emerging interesting phenomena in structurally simple cobalt oxides with spin-charge-lattice coupling. $\text{Pr}_{0.50}\text{Ca}_{0.50}\text{CoO}_3$ (PCCO) and $\text{Pr}_{0.50}\text{Sr}_{0.50}\text{CoO}_3$ (PSCO) exhibit distinct anomalous structural and magnetic properties, which have been largely controversial.¹⁻⁹

Metallic half-doped $\text{Pr}_{0.50}\text{Ca}_{0.50}\text{CoO}_3$ undergoes a non-conventional metal-insulator and concomitant Co spin-state transition at $T_{\text{MI}} \sim 80$ K. Below that temperature the insulating state is stabilized by electron transfer from Pr to Co sites.¹⁻⁶ This exceptional electronic mechanism in PCCO and other $(\text{Pr},\text{R})_{1-x}\text{Ca}_x\text{CoO}_3$ cobaltites (R: rare-earth or lanthanide) with *Pnma* symmetry seems to be based on the contraction of selected Pr-O bonds⁴ that generate a first-order Pr^{3+} to Pr^{4+} valence shift at T_{MI} , accompanied by the stabilization of the Co^{3+} LS state.^{3,6}

$\text{Pr}_{0.50}\text{Sr}_{0.50}\text{CoO}_3$ is metallic (*Imma* symmetry) and presents two transitions on cooling.⁷ First, it becomes ferromagnetic (FM) below $T_{\text{C}}=230$ K, then it exhibits a second unexpected transition at $T_{\text{S}}\sim 120$ K which has not been observed with other rare-earth cations. It was first reported by Mahendiran *et al*⁷ from magnetization and specific heat measurements, and produces an appealing step-like behavior in the magnetization that has been attributed to possible changes in the magnetocrystalline anisotropy axis.^{8,9} Neutron studies did not observe any evidence for antiferromagnetism.

The structural properties of $\text{Pr}_{0.50}\text{Sr}_{0.50}\text{CoO}_3$ indicate a change in the crystal symmetry at T_S where the emerging low temperature monoclinic phase could be related to changes in the magnetic easy-axis.^{8,10,11} Troyanchuk *et al*¹⁰ and later Leighton *et al*⁸ underlined the possible importance of the Pr $4f$ – O $2p$ hybridization for the transition. Nevertheless, there is no convincing explanation about its origin yet, and different hypothetical scenarios have been invoked.⁸⁻¹¹ Among others, orbital ordering or orbital state changes, spin-state changes in Co^{3+} ions, hybridization between Pr- $4f$ orbital and O- $2p$ orbitals, etc.

We consider that the scenario of a large hybridization between Pr- $4f$ and O- $2p$ states at the MIT in PCCO and other $(\text{Pr,R})_{1-x}\text{Ca}_x\text{CoO}_3$ cobaltites (R: rare-earth or lanthanide) justifies similar exploratory studies across this coupled structural/magnetocrystalline anisotropy transition in PSCO. Here we present a comparative study of the Ca and Sr compounds that gives support to this scenario.

II. EXPERIMENTAL DETAILS

Samples of $\text{Pr}_{0.50}\text{Ca}_{0.50}\text{CoO}_3$ and $\text{Pr}_{0.50}\text{Sr}_{0.50}\text{CoO}_3$ were prepared in polycrystalline form following standard solid-state reaction methods, from the intimate mixture of high purity precursor oxides (Co_3O_4 and Pr_6O_{11} and CaCO_3 or SrCO_3). Details about the sintering conditions used for the former were described in ref.¹. In order to reach the optimal oxygenation it was necessary to finally treat PCCO under high oxygen pressure (at 900°C and $P_{\text{O}_2}=200$ bar during 14 hours, and at 475°C and $P_{\text{O}_2}=150$ bar during 6 hours). For PSCO sample, after several intermediate-stage sintering, the last sintering temperature was 1170°C , under oxygen atmosphere. PSCO samples were then slowly cooled down to room temperature in the presence of oxygen. Sample characterization included x-ray and neutron diffraction. X-ray powder diffraction using a Siemens D-5000 diffractometer showed both samples free from impurities. The oxygen content was checked through Rietveld refinement

of neutron powder diffraction data, confirming that both samples are stoichiometric. Neutron powder diffraction (NPD) measurements were done at the Institute Laue-Langevin (ILL, Grenoble) using D20 diffractometer and $\lambda = 1.87 \text{ \AA}$ (in high resolution mode). NPD diffractograms have been refined by the Rietveld method using FullProf suite of programs [12]. Magnetic and resistivity measurements (by the four-probe method) were performed using the Physical Properties Measuring System and SQUID from Quantum Design.

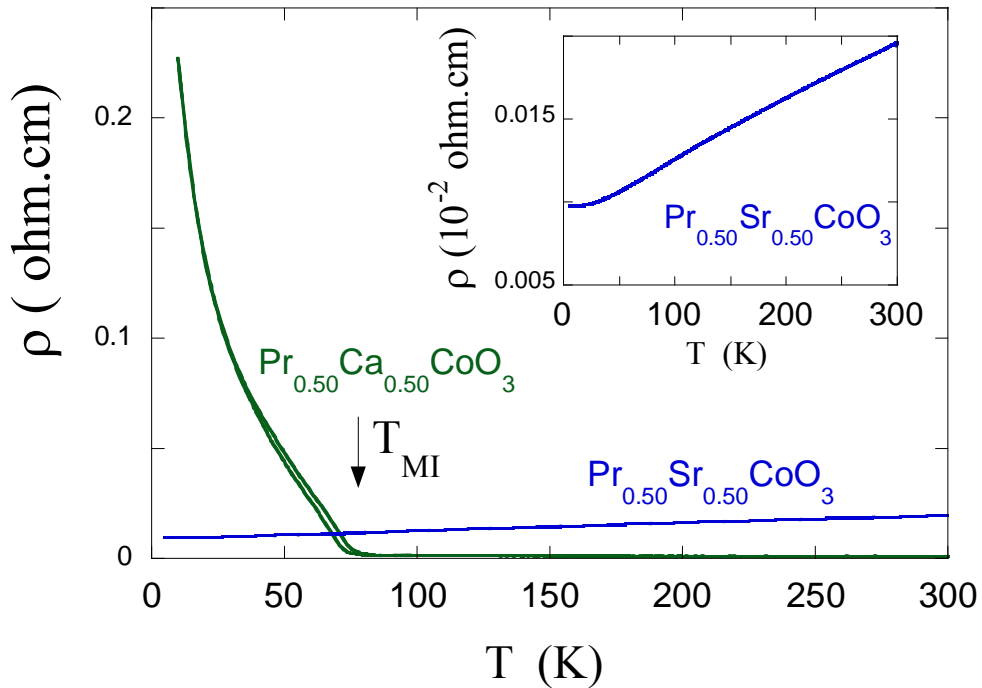


FIG. 1 (Color online) Temperature dependence of the electrical resistivity (without applied field) for $\text{Pr}_{0.50}\text{Ca}_{0.50}\text{CoO}_3$ and $\text{Pr}_{0.50}\text{Sr}_{0.50}\text{CoO}_3$. Inset: detailed for the Sr compound.

III. RESULTS AND DISCUSSION

The electrical resistivity of ceramic PSCO and PCCO samples is compared in Fig. 1. The insulating behaviour of PCCO below $T_{\text{MI}} \sim 75 \text{ K}$ contrasts with the metallicity of PSCO down to the lowest temperature. The low temperature transition in the Sr-based compound does not

modify its metallic character, and its resistivity curve does not show neither any visible anomaly around T_s .

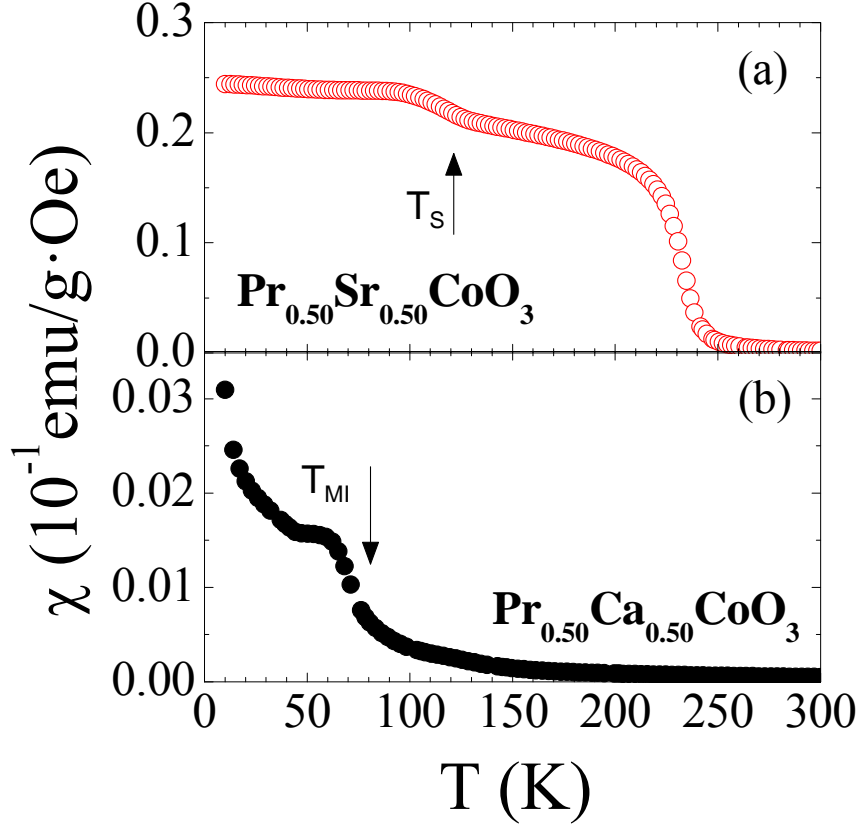


FIG. 2 (Color online) Temperature dependence of the magnetic susceptibility at measuring field of 0.1T (field-cooled) for (a) $\text{Pr}_{0.50}\text{Sr}_{0.50}\text{CoO}_3$ and (b) $\text{Pr}_{0.50}\text{Ca}_{0.50}\text{CoO}_3$.

As shown in Fig. 2 the magnetization of these cobaltites is very different, even in the metallic zone. The Curie temperature of PSCO is ~ 230 K and PCCO does not present spin-order (the stabilization of the Co^{3+} LS state in the insulating phase explains the absence of long-range magnetic order at low temperatures⁶). The step in the magnetization of PSCO around $T_s \approx 120$ K is the most characteristic feature of the magnetostructural transition. We recall that the upward step shown in the figure (0.1T field cooled on warming) changes into a downward step for $\mu_0 H \leq 50$ mT^{7,8} (an intrinsic/reproducible feature of this transition).

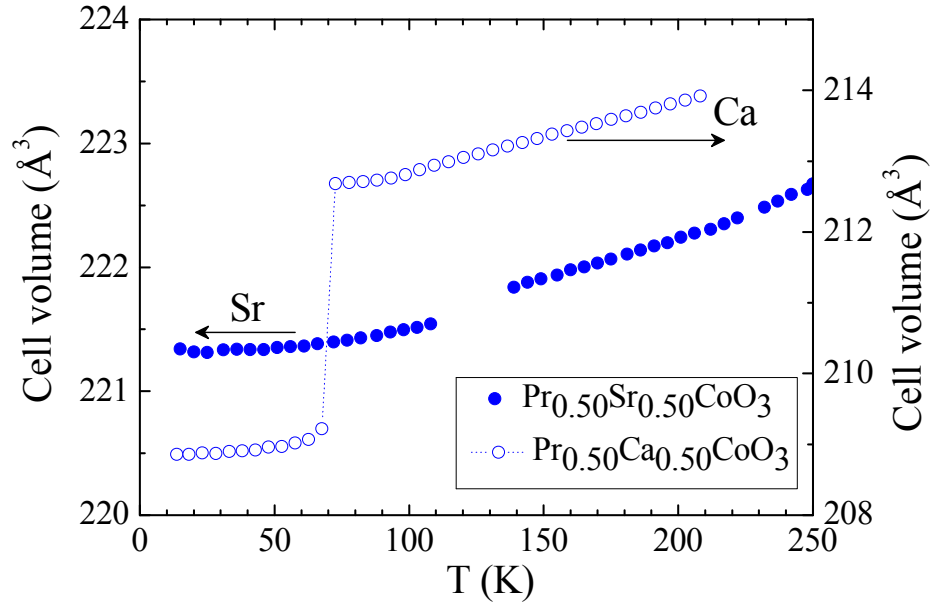


FIG. 3 (Color online) Thermal evolution of the volume for $\text{Pr}_{0.50}\text{Sr}_{0.50}\text{CoO}_3$ (left axis) and $\text{Pr}_{0.50}\text{Ca}_{0.50}\text{CoO}_3$ (right axis).

The evolution as a function of temperature of the unit cell volumes for PCCO and PSCO samples, determined from diffraction data, is plotted in Fig. 3.¹³ A contraction of the cell volume was detected in PSCO below T_S . Note that, as this figure clearly shows, the volume change is very small (0.1%) compared to the 2% volume contraction in PCCO when enters the insulating phase. Rietveld analysis of our NPD data from PSCO confirm a structural transition from orthorhombic ($Imma$) to monoclinic symmetry ($I2/a$) at T_S .¹⁴ Using these space groups to refine the diffraction patterns collected, respectively, at both sides of the transition, we have explored the evolution of main structural parameters. A complete description of the three successive crystal structures ($R-3c > Imma > I2/a$) in $\text{Pr}_{0.50}\text{Sr}_{0.50}\text{CoO}_3$ decreasing temperature and more details of the respective transformations at 315 K and 120 K can be found in ref.¹⁴ Here we will mainly focus the study on the changes observed around Pr atoms, which will be compared to corresponding changes previously observed in PCCO, where the active participation of Pr 4f electrons was proved to produce

the cell volume reduction and metal-insulator transition. In other words, a remarkable Pr-O bond shortening in PCCO was found to induce the Pr^{3+} to Pr^{4+} valence drift at the MIT. In the crystal structure, Pr atoms (at R-site) are coordinated by 8+4 oxygen atoms. Given the eight nearest neighbor oxygen shell around R-site, we have derived the average $\langle\text{R-O}\rangle^{\text{VIII}}$ bond distance and its temperature evolution. So, Fig. 4 displays a comparison of the evolution of $\langle\text{R-O}\rangle^{\text{VIII}}$ for the two halfdoped cobaltites. Interestingly, despite the small volume contraction in PSCO, the figure reveals that there is a very strong shortening of the average $\langle\text{R-O}\rangle^{\text{VIII}}$ bondlength in PSCO at T_{S} . The sudden change in $\langle(\text{Pr,Sr})\text{-O}\rangle^{\text{VIII}}$ ($\sim -4\%$) is around twice the size of the average bond contraction in PCCO. This finding is consistent with previous evidences suggesting the active participation of Pr electrons in the magnetostructural transition. In addition, the inset of Fig. 5 shows that the volume of the CoO_6 octahedra is hardly modified across the transition. This corroborates the idea that the changes could be induced by the competition between Pr-O covalent bonding and the tilting of the octahedra in the skeleton of corner-sharing CoO_6 units.

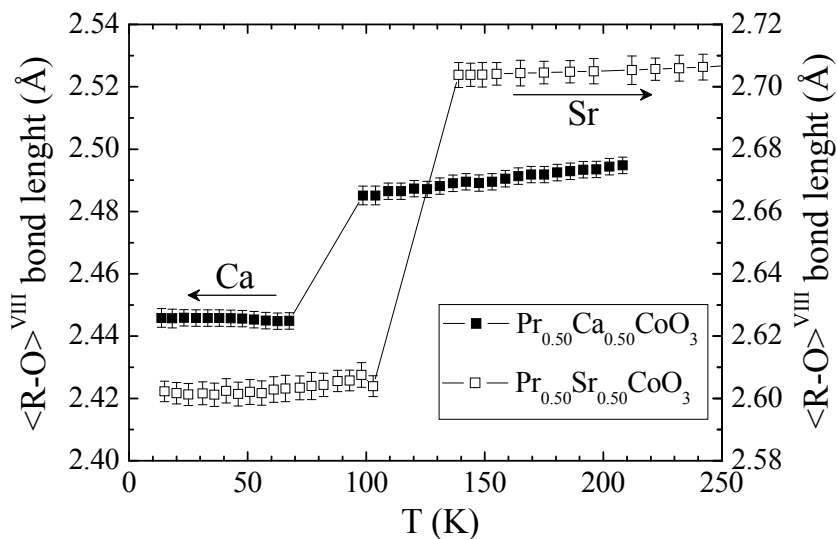


FIG. 4. Temperature dependence of the average (Pr,A)-O bond distance (VIII-coord., A:Ca or Sr) for $\text{Pr}_{0.5}\text{Ca}_{0.5}\text{CoO}_3$ (left axis) and $\text{Pr}_{0.5}\text{Sr}_{0.5}\text{CoO}_3$ (right axis).

The eight nearest neighbor oxygens around Pr consist of four apical (O1) and four basal (O2) oxygen atoms.^{4,8,14} We found that, as Leighton *et al* proposed in Ref. ⁸, there are three inequivalent Pr-O1 bondlengths in the Pr-O planes above T_S : R-O1=2.96 Å, 2.47 Å and ~2.70 Å [x2]. On cooling below the transition temperature T_S , R-O1 distances become practically identical and adopt the average value ~2.69 Å. Consequently, in view of the large drop in $\langle R-O \rangle^{VIII}$, the largest changes must involve O2 oxygens in the basal plane of the octahedra. In order to confirm this result and get further insight we have determined the evolution of the average distance $\langle R-O2 \rangle^{VIII}$, considering only basal oxygens in the first coordination sphere. The evolution of the bondlength $\langle R-O2 \rangle^{VIII}$ in the perovskite is depicted in Fig. 5. This figure clearly evidences that the half-doped Sr cobaltite undergoes a very large Pr-O2 bond contraction during the magnetostructural changes at T_S . The change observed in the figure comparing both sides of the transition is $\Delta d \sim -7\%$.

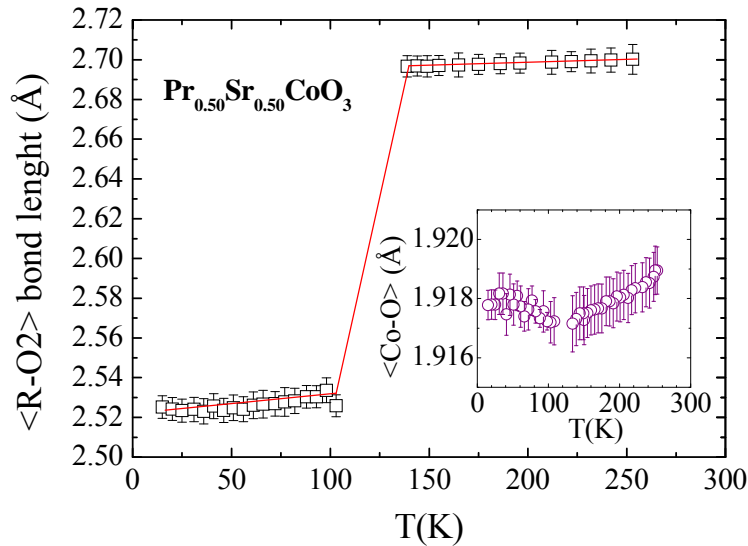


FIG. 5 (Color online) (a) Evolution with temperature of the average (Pr,Sr)-O2 bond distance (VIII-coord.) across the second magnetic transition at T_S in $\text{Pr}_{0.50}\text{Sr}_{0.50}\text{CoO}_3$. The solid lines are guides to the eye. The inset shows the average Co-O bond distance of the CoO_6 octahedra.

In view of these results, which points towards an active role of Pr through a large hybridization between Pr-4*f* and O-2*p* states, we prepared a half-doped composition without Pr. A $(\text{Nd}_{2/3}\text{La}_{1/3})_{0.50}\text{Sr}_{0.50}\text{CoO}_3$ ceramic sample was synthesized following the same procedure as for $\text{Pr}_{0.50}\text{Sr}_{0.50}\text{CoO}_3$. This new composition was chosen with the aim of testing and searching an independent validation of our structural data interpretation. Thus, the interest of this composition is that it does not contain Pr atoms but the average ionic radius at R site is identical (1.193 Å) to $\text{Pr}_{0.50}\text{Sr}_{0.50}\text{CoO}_3$. $(\text{Nd}_{2/3}\text{La}_{1/3})_{0.50}\text{Sr}_{0.50}\text{CoO}_3$ was found to be metallic and its magnetization is plotted in Fig. 6 (measured after field-cooling at 0.1 T). It is found that the ferromagnetic order of Co moments takes place at about the same Curie temperature as for $\text{Pr}_{0.50}\text{Sr}_{0.50}\text{CoO}_3$. Though, the key observation is the absence of the magnetostructural transition in this cobaltite without praseodymium at the R site. In Fig. 6 the downturn in the magnetization below 60 K simply shows the polarization of Nd moments by the Co spins.

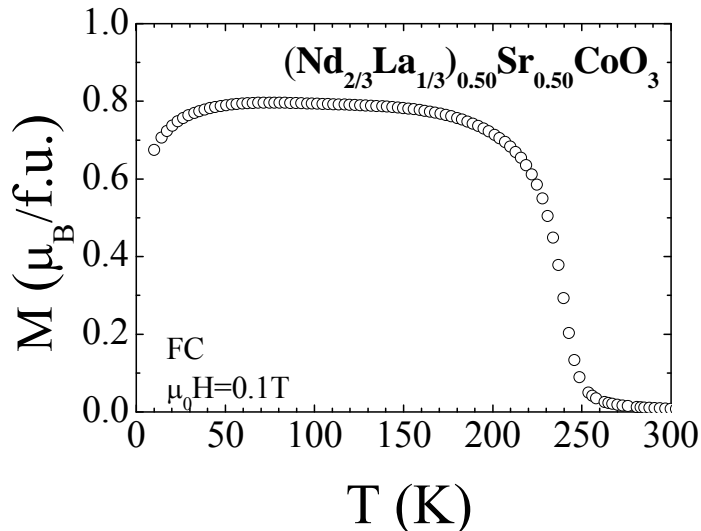


FIG. 6 Magnetic susceptibility for $(\text{Nd}_{2/3}\text{La}_{1/3})_{0.50}\text{Sr}_{0.50}\text{CoO}_3$ (field-cooled, measured on heating under 0.1T), showing a single high-temperature ferromagnetic transition from Co.

IV. CONCLUSION

In summary, a strong contraction of some Pr-O bonds in $\text{Pr}_{0.50}\text{Sr}_{0.50}\text{CoO}_3$ at the “so called” magnetocrystalline anisotropy transition points towards an active participation of Pr atoms at T_S . Despite the evolution of the Pr-O network strongly differs in $\text{Pr}_{0.50}\text{Sr}_{0.50}\text{CoO}_3$ and $\text{Pr}_{0.50}\text{Ca}_{0.50}\text{CoO}_3$ compounds, both have in common a prominent contraction of some Pr-O bonds. An independent corroboration of the active role of Pr *4f* electrons was obtained from an evaluation of the properties of the $(\text{Nd}_{2/3}\text{La}_{1/3})_{0.50}\text{Sr}_{0.50}\text{CoO}_3$ cobaltite. We confirmed that the low temperature magnetostructural transition is suppressed in this Sr-based halfdoped perovskite with no praseodymium, although it presents an identical hole doping and the same average cationic radius at A site as $\text{Pr}_{0.50}\text{Sr}_{0.50}\text{CoO}_3$.

The stability of the valence of praseodymium ions in $\text{Pr}_{0.50}\text{Sr}_{0.50}\text{CoO}_3$ must be clarified and further investigated using additional techniques such as X-ray absorption spectroscopy. New experiments must elucidate whether the observations reported here at the magnetostructural transition are the expression of changes in the oxidation state of Pr^{3+} ions or just a consequence of changes in the strength of the Pr-O covalent bonding.

ACKNOWLEDGMENTS

We thank financial support from MINECO (Spanish government) under projects MAT2009-09308, MAT2012-38213-C02-02 and CSD2007-00041 (NANOSELECT), and the ILL for granting beamtime. J.P-P thanks CSIC for JAE-Pre contract.

References

- ¹ A. J. Barón-González, C. Frontera, J. L. García-Muñoz, J. Blasco, and C. Ritter, *Phys. Rev. B* 81, 054427 (2010).
- ² J. Hejtmanek, E. Šantavá, K. Knížek, M. Maryško, Z. Jiráček, T. Naito, H. Sasaki, and H. Fujishiro, *Phys. Rev. B* 82, 165107 (2010).
- ³ K. Knizek, J. Hejtmanek, P. Novák, and Z. Jiráček, *Phys. Rev. B* 81, 155113 (2010)

- ⁴ J. L. García-Muñoz, C. Frontera, A. J. Barón-González, S. Valencia, J. Blasco, R. Feyerherm, E. Dudzik, R. Abrudan, and F. Radu, *Phys. Rev. B* 84, 045104 (2011)
- ⁵ J. Herrero-Martín, J. L. García-Muñoz, S. Valencia, C. Frontera, J. Blasco, A. J. Barón-González, G. Subías, R. Abrudan, F. Radu, E. Dudzik, and R. Feyerherm, *Phys. Rev. B* 84, 115131 (2011).
- ⁶ J. Herrero-Martín, J. L. García-Muñoz, K. Kvashnina, E. Gallo, G. Subías, J. A. Alonso, and A. J. Barón-González, *Phys. Rev. B* 86, 125106 (2012).
- ⁷ R. Mahendiran and P. Schiffer, *Phys. Rev. B* 68, 024427 (2003).
- ⁸ C. Leighton, D. D. Stauffer, Q. Huang, Y. Ren, S. El-Khatib, M. A. Torija, J. Wu, J. W. Lynn, L. Wang, N. A. Frey, H. Srikanth, J. E. Davies, Kai Liu, and J. F. Mitchell, *Phys. Rev. B* 79, 214420 (2009).
- ⁹ N. A. Frey Huls, N. S. Bingham, M. H. Phan, H. Srikanth, D. D. Stauffer and C. Leighton, *Phys. Rev. B* 83, 024406 (2011).
- ¹⁰ I. O. Troyanchuk, D. V. Karpinskii, A. N. Chobot, D. G. Voitsekhovich, and V. M. Bobryanskii, *JETP Lett.* 84, 151 (2006).
- ¹¹ A. M. Balagurov, I. A. Bobrikov, V. Y. Pomjakushin, E. V. Pomjakushina, D. V. Sheptyakov and I. O. Troyanchuk, *JETP Lett.* 93, 263 (2011).
- ¹² J. Rodríguez-Carvajal, *Physica B* 192, 55 (1993).
- ¹³ The structural evolution of our PCCO sample was extensively reported in refs. 1 and 4. The structural data from PCCO used here have been taken and adapted from these references.
- ¹⁴ J. Padilla-Pantoja, J.L. García-Muñoz and J. Herrero-Martín. Submitted.

Figure Captions

FIG. 1 (Color online) Temperature dependence of the electrical resistivity (without applied field) for $\text{Pr}_{0.50}\text{Ca}_{0.50}\text{CoO}_3$ and $\text{Pr}_{0.50}\text{Sr}_{0.50}\text{CoO}_3$. Inset: detailed for the Sr compound.

FIG. 2 (Color online) Temperature dependence of the magnetic susceptibility at measuring field of 0.1T (field-cooled) for (a) $\text{Pr}_{0.50}\text{Sr}_{0.50}\text{CoO}_3$ and (b) $\text{Pr}_{0.50}\text{Ca}_{0.50}\text{CoO}_3$.

FIG. 3 (Color online) Thermal evolution of the volume for $\text{Pr}_{0.50}\text{Sr}_{0.50}\text{CoO}_3$ (left axis) and $\text{Pr}_{0.50}\text{Ca}_{0.50}\text{CoO}_3$ (right axis).

FIG. 4. Temperature dependence of the average (Pr,A)-O bond distance (VIII-coord., A:Ca or Sr) for $\text{Pr}_{0.50}\text{Ca}_{0.50}\text{CoO}_3$ (left axis) and $\text{Pr}_{0.50}\text{Sr}_{0.50}\text{CoO}_3$ (right axis).

FIG. 5 (Color online) (a) Evolution with temperature of the average (Pr,Sr)-O2 bond distance (VIII-coord.) across the second magnetic transition at T_S in $\text{Pr}_{0.50}\text{Sr}_{0.50}\text{CoO}_3$. The solid lines are guides to the eye. The inset shows the average Co-O bond distance of the CoO_6 octahedra.

FIG. 6 Magnetic susceptibility for $(\text{Nd}_{2/3}\text{La}_{1/3})_{0.50}\text{Sr}_{0.50}\text{CoO}_3$ (field-cooled, measured on heating under 0.1 T), showing a single high-temperature ferromagnetic transition from Co.